Electron Tunneling in Substrate-Reduced Trimethylamine Dehydrogenase: Kinetics of ElectronTransfer and Analysis of the Tunneling Pathway†

Emma K. Wilson,‡ F. S. Mathews,§ Leonard C. Packman,‡ and Nigel S. Scrutton*,‡

Cambridge Centre for Molecular Recognition, Department of Biochemistry, University of Cambridge, Cambridge CB2 1QW, U.K., and Department of Biochemistry, Washington University School of Medicine, St. Louis, Missouri 63110

Received July 6, 1994; Revised Manuscript Received November 10, 1994®

ABSTRACT: The reoxidation of substrate-reduced trimethylamine dehydrogenase by the artificial electron acceptor ferricenium hexafluorophosphate was studied by stopped-flow spectroscopy. The rate constants for the two sequential one-electron transfers from the reduced 4Fe-4S center to ferricenium ions were measured, the first (k_a = 49 s^{-1}) being about 7 times greater than the second (k_b = 7.3 s^{-1}) at 20 °C and neutral pH. The temperature dependence of the second electron transfer was studied over the range 10−40 °C, and the rate constant ranged from 5.7 to 19.2 s^{-1}. Analysis of the temperature perturbation of k_b by Marcus theory yielded values for the reorganizational energy of 1.95 eV and the electronic coupling matrix element of 0.26 cm^{-1}. An electron tunneling pathway distance of 13 ± 0.7 Å was calculated which correlates with the shortest pathway measured from the 4Fe-4S center to the protein surface using the crystallographic coordinates of trimethylamine dehydrogenase. Tyr-442 is implicated in facilitating electron transfer from the enzyme to ferricenium ions. The data suggest a location for the docking site on the surface of trimethylamine dehydrogenase for the physiological electron acceptor (ETF).

Electron transfer is the simplest of chemical reactions. Unlike those chemical reactions which involve the making and breaking of bonds, biological electron transfer reactions are not localized and may take place over large distances, typically 10−20 Å. Consequently, orbital overlap between the donor and acceptor sites is very weak. Despite this weak overlap, electron transfer reactions can be extremely fast, and reactions exhibit remarkable specificity. In any theory which describes electron transfer, several basic questions need to be addressed: for example, how does the protein structure between redox centers influence the physical factors that drive electron transfer, and what are the roles played by the redox centers and the solvent in the transfer event? Recently, there has been renewed interest in the physical factors governing electron transfer reactions due mainly to the extension into the biological arena of ideas initially developed for chemical systems [for a review, see Farid *et al.* (1993)].

Methylotrophic bacteria provide an abundant source of electron transfer proteins which are required for the dissimilation of substrates lacking carbon−carbon bonds. One such protein, trimethylamine dehydrogenase, is a complex iron−sulfur flavoprotein whose action is to convert trimethylamine into dimethylamine and formaldehyde (Steenkamp & Mallinson, 1976):

$$(CH_3)_3N + H_2O \rightleftharpoons (CH_3)_2NH + CH_2O + 2e^- + 2H^+$$

In vivo, the electrons derived from this conversion are passed to an electron transfer flavoprotein, thereby regenerating the oxidized form of the enzyme (Steenkamp & Gallup, 1978). Trimethylamine dehydrogenase is a symmetrical dimer of subunits (M_r 81623) each of which contains a single [4Fe-4S] cluster (Hill et al., 1977) and one FMN prosthetic group attached to the protein by a unique 6*S*-cysteinyl FMN bond (Steenkamp et al., 1978; Kenney et al., 1978). The enzyme also binds ADP (Lim et al., 1988), but the function of this third cofactor remains obscure, although it probably represents the vestigial remains of a dinucleotide-binding site (Lim et al., 1988; Scrutton, 1994). The crystal structure of the enzyme is solved at 2.4-Å resolution (Lim et al., 1986) and has recently been refined (F. S. Mathews and S. A. White, unpublished work). The enzyme comprises three domains, the first (amino terminal) folded as an α/β-barrel domain. The active site of the enzyme resides in this domain, and it contains the site for attachment of the covalently linked FMN prosthetic group. The other two domains comprise five-stranded parallel β-sheets flanked by helices and other structural elements, and they are similar in fold to the two dinucleotide-binding domains found in glutathione reductase (Lim et al., 1988). The iron−sulfur cluster is positioned at the junction between the α/β-barrel domain and the smaller C-terminal domains. From the high-resolution electron density map, it has been possible to derive a hypothetical amino acid sequence for the enzyme, and this has recently been substantiated by chemical sequencing methods (Barber et al., 1991) and DNA sequencing of the cloned *tmd* gene encoding trimethylamine dehydrogenase (Boyd et al., 1992).

Initial reduction of trimethylamine dehydrogenase by substrate is at the barrel-bound flavin and is very rapid ($t_{1/2}$ < 2ms at pH 7.7 with 500 μM trimethylamine; Steenkamp et al., 1978). This rapid reduction is followed by a kinetically slower phase ($t_{1/2}$ about 80 ms) giving rise to full development of a g = 4 EPR signal and spectral changes observed at 365 and 520 nm. This slower phase coincides with the intramolecular transfer of one electron from the flavin to

† This work was supported by a grant from the Leverhulme Trust (to N.S.S and L.C.P) and the Royal Society (to N.S.S.). E.K.W. was supported by a MRC research studentship.

* To whom correspondence should be addressed.
‡ University of Cambridge.
§ Washington University School of Medicine.

® Abstract published in *Advance ACS Abstracts,* February 1, 1995.

0006-2960/95/0434-2584$09.00/0

oxidized iron−sulfur. The observed rate constant for the intramolecular electron transfer in dithionite-reduced enzyme is about 100-fold greater than k_{cat} (approx. 10 s^{-1}; see below) when ferricenium hexafluorophosphate acts as the terminal artificial electron acceptor, and therefore, intramolecular electron transfer is not intrinsically rate-limiting in overall catalysis (Rohlfs & Hille, 1991). The part of the reaction sequence which has not been investigated in any detail is the transfer of electrons from the iron−sulfur center to artificial electron acceptors, e.g., ferricenium ions. This part of the reaction is the primary focus of this paper.

The factors governing the rate of biological electron transfer are predicted by Marcus theory (Marcus & Sutin, 1985). The theory relates the electron transfer rate (k_{ET}) as a function of free energy change ($\Delta G°$), temperature (T), the electronic coupling matrix element (H_{AB}), and the sum of the inner sphere (higher vibrational frequency of immediate ligands of the redox center) and outer sphere (lower vibrational frequency of solvent and protein atoms) reorganizational energies (λ). The equation relating the nuclear and electronic factors to the rate of electron transfer is

$$k_{ET} = \frac{4\pi^2 H^2_{AB}}{h(4\pi\lambda RT)^{1/2}} e^{-(\Delta G°+\lambda)^2/4\lambda RT} \quad (1)$$

and comprises a classical component associated with nuclear motion and a quantum mechanical component (H^2_{AB}) associated with electron tunneling. R is the gas constant, h is Planck's constant, and T is the absolute temperature. The tunneling matrix element (H_{AB}) represents the probability of electron transfer at the point of intersection of the multidimensional potential energy curves for the reactants (electron resident on the donor redox site), and products (electron resident on the acceptor redox site) and its value depends on the distance (r) between the two redox centers. In systems with homogeneous bridging material, its value decreases exponentially as a function of tunneling distance (r) and is modified by a coefficient β (the electronic decay factor), as predicted by Gamow's tunneling equation,

$$H_r^2 = H_o^2 e^{-\beta r} \quad (2)$$

where H_o is the tunnelling matrix element at van der Waals separation and H_r is the tunnelling matrix element at separation r. The precise value of β may change throughout the tunneling pathway and depends on various factors, for example, whether the tunneling pathway is made up of covalent, hydrogen-bond, or "through space" connectivities (Beratan et al., 1991, 1992). Since in proteins tunneling pathways will usually involve all three types of connectivity, the β value is often approximated to 1.4 $Å^{-1}$ (Moser et al., 1992), which is intermediate in value for systems using covalently linked pathways ($\beta = 0.7$ $Å^{-1}$) and those in which tunneling pathways pass through vacuum ($\beta = 2.8$ $Å^{-1}$). From Marcus theory, electron transfer rates are predicted to depend on distance (r) by the following relationship:

$$k_{ET} = k_o e^{-\beta(r-r_o)} e^{-(\Delta G°+\lambda)^2/4\lambda RT} \quad (3)$$

where k_o is the characteristic frequency of the nuclei, which is assigned a value of 10^{13} s^{-1} (Marcus & Sutin, 1985; Rees & Farrelly, 1990), and r_o represents the van der Waals distance (3 Å). Using Marcus theory, we report here an analysis of the electron transfer kinetics of substrate-reduced trimethylamine dehydrogenase to the artificial electron acceptor ferricenium hexafluorophosphate. From these experiments, we have calculated values for the electron tunneling pathway distance (r), the electronic coupling matrix element (H_{AB}), and the reorganizational energy (λ) associated with electron transfer. The results are discussed with reference to the high-resolution crystal structure of trimethylamine dehydrogenase, and a possible tunneling pathway is identified.

EXPERIMENTAL PROCEDURES

Purification of trimethylamine dehydrogenase was as described by Steenkamp and Mallinson (1976) except that the last gel filtration step was replaced by a hydrophobic interaction chromatographic separation using phenyl-Sepharose (Scrutton et al., 1994). Enzyme concentrations were determined from the 443-nm absorbance of oxidized enzyme using an extinction coefficient of 27.3 mM^{-1} cm^{-1} in 20 mM potassium phosphate buffer, pH 7.0. Ferricenium hexafluorophosphate was synthesised as described by Lehman et al. (1990), and concentrations of stock solutions were determined from the 300-nm absorbance of oxidized ferricenium hexafluorophosphate using an extinction coefficient of 4300 M^{-1} cm^{-1}. All chemicals were of analytical grade wherever possible. Glass-distilled water was used throughout.

Steady-state kinetic measurements were performed with a 1-cm light path in a final volume of 1 mL. The desired concentrations of trimethylamine and ferricenium hexafluorophosphate were obtained by making microliter additions from stock solutions to the assay mix. Reactions were started by the addition of enzyme, and the decrease in absorbance at 300 nm due to the reduction of ferricenium ions was measured using a Hewlett-Packard 8452A single-beam diode-array spectrophotometer. Aerobic reductive titrations were performed by measuring the spectrum of trimethylamine dehydrogenase using a Kontron 930 uvikon spectrophotometer following successive additions of trimethylamine contained in 20 mM potassium phosphate buffer, pH 7.0. The oxidase rate of substrate-reduced trimethylamine dehydrogenase was determined by measuring the spectrum of the enzyme as a function of time. The increase in absorbance at 443 nm was used to indicate the recovery of the oxidized enzyme species.

Rapid reaction studies of electron transfer from substrate-reduced trimethylamine dehydrogenase to ferricenium hexafluorophosphate were monitored using an Applied Photophysics stopped-flow spectrophotometer (SF. 17MV). Data were collected and analyzed using nonlinear least squares regression analysis on an Archimedes 410-1 microcomputer. Experiments were carried out by mixing trimethylamine dehydrogenase in 20 mM potassium phosphate buffer, pH 7.0 (reduced with a stoichiometric amount of trimethylamine) with an equal volume of ferricenium hexafluorophosphate contained in the same buffer. Reduction of ferricenium ions by substrate-reduced trimethylamine dehydrogenase was monitored at 347 nm where an isosbestic point for trimethylamine dehydrogenase exists (see below). Nonlinear least squares regression analysis was used to fit temperature

perturbation data to the classical Marcus equations using the Kaleidograph software program (Abelbeck software).

RESULTS

Steady-State Kinetic Analyses. As a guide to stopped-flow studies, steady-state kinetic constants were evaluated from reactions performed at 20 °C in 20 mM potassium phosphate buffer, pH 7.0. The apparent K_m for ferricenium hexafluorophosphate and the apparent k_{cat} were determined using a fixed concentration of trimethylamine (50 μM). Higher concentrations of trimethylamine lead to substrate inhibition of the enzyme (Steenkamp & Gallup, 1978), and therefore, the substrate concentration chosen is only about 2.5-fold higher in concentration than the apparent K_m for trimethylamine (17 μM; Scrutton et al., 1994) determined at 200 μM ferricenium hexafluorophosphate. Under these conditions, an apparent K_m of 28 ± 2.3 μM for ferricenium hexafluorophosphate and an apparent k_{cat} of 9.2 ± 0.3 s^{-1} were measured. The value of k_{cat} is lower than the 30-s^{-1} value previously reported by Scrutton et al. (1994). The reason for the difference lies in the nature of the nonlinear least squares fit and the conditions under which it was determined. The higher value of 30 s^{-1} was measured by varying the trimethylamine concentration at a fixed concentration of ferricenium hexafluorophosphate (200 μM). The data were then fitted to a rectangular hyperbola, which does not take account of substrate inhibition by trimethylamine. The fitting procedure therefore overestimates k_{cat}. Also, the analyses were performed under conditions of optimum pH (pH 7.5) at 30 °C, whereas the data reported here were measured at pH 7.0 and 20 °C. The steady-state analyses were performed at neutral pH because the redox potentials of the 4Fe-4S center and ferricenium ions were previously measured at pH 7.0.

Oxidase Activity of Trimethylamine Dehydrogenase. Reductive titrations of trimethylamine dehydrogenase using trimethylamine as the reductant were performed under aerobic conditions at 20 °C in 20 mM potassium phosphate buffer, pH 7.0. The titration revealed the presence of an isosbestic point at 347 nm (Figure 1) as seen previously (Steenkamp et al., 1978), and this wavelength was chosen for the stopped-flow kinetic analyses described below. At 347 nm, there is a change in the extinction coefficient ($\Delta\epsilon$ = 485 M^{-1} cm^{-1}) for ferricenium hexafluorophosphate on being converted from the oxidized to the reduced form (Lehman et al., 1990). Following stoichiometric reduction of the enzyme with trimethylamine, the oxidase activity of the enzyme was determined by repeatedly measuring the absorption spectrum of the enzyme from 800 to 300 nm. The rate of recovery of the oxidized enzyme was calculated by monitoring the change in absorbance at 443 nm (Figure 1, inset). Reoxidation of the enzyme was relatively slow (half-life about 50 min). In the stopped-flow experiments, the time interval between enzyme reduction and injection of samples into the reaction chamber was on the order of a few minutes, and reoxidation of substrate-reduced trimethylamine dehydrogenase is negligible in this time period. Consequently, the need to use anaerobic conditions in the stopped-flow experiments was negated, and all analyses were conducted under aerobic conditions.

Stopped-Flow Kinetic Analyses. Pseudo-first-order reactions were performed at different temperatures using a fixed concentration (500 μM) of ferricenium hexafluorophosphate and a fixed subunit concentration of substrate-reduced trimethylamine dehydrogenase (41 μM). The concentration of trimethylamine required to reduce stoichiometrically trimethylamine dehydrogenase is similar to the concentration of trimethylamine (50 μM) used in the steady-state kinetic analyses (see above). It was assumed that the reduction of ferricenium hexafluorophosphate by substrate-reduced trimethylamine dehydrogenase proceeded by the simple kinetic model (Scheme 1) in which two-electron-reduced trimethylamine dehydrogenase reacts in a sequential manner with oxidized ferricenium hexafluorophosphate present at saturating concentrations (~20 K_m). For simplicity, binding steps are omitted in Scheme 1.

Given the sluggish nature of electron transfer from substrate-reduced trimethylamine dehydrogenase to ferricenium hexafluorophosphate (see below), in this scheme it is assumed that the rapid equilibrium assumption applies and that complex formation of the reacting species occurs in a fast diffusion-controlled process followed by slow rate determining electron transfer steps. The difference in redox potential (0.278 V; see below) between the 4Fe-4S center

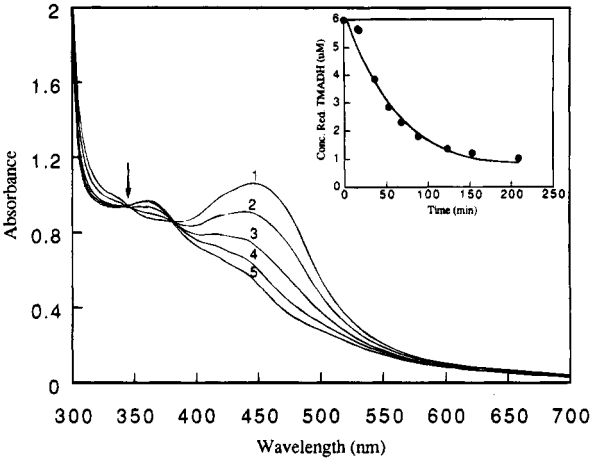

FIGURE 1: Reductive titrations of trimethylamine dehydrogenase with trimethylamine. Titrations were performed under aerobic conditions in 20 mM potassium phosphate buffer, pH 7.0. Trimethylamine dehydrogenase concentration is 41 μM. The isosbestic point at 347 nm is indicated by a vertical arrow. (1) Oxidized enzyme; (2) enzyme reduced with 0.25 mol equiv of trimethylamine; (3) enzyme reduced with 0.5 mol equiv of trimethylamine; (4) enzyme reduced with 0.75 mol equiv of trimethylamine; (5) enzyme reduced with 1.0 mol equiv of trimethylamine. Inset: Plot of concentration of reduced trimethylamine dehydrogenase against time for the aerobic recovery of the oxidized form of trimethylamine dehydrogenase. Enzyme (6 μM) was stoichiometrically reduced with trimethylamine, and the spectrum of the enzyme was recorded at various time intervals following reduction from which the increase in absorbance at 443 nm was determined. The increase in absorbance at 443 nm was used to calculate the rate of recovery of the oxidized enzyme.

Scheme 1

$$\text{TMADH(2e).FPF}_6 \underset{k_a'}{\overset{k_a}{\rightleftharpoons}} \text{TMADH(e).FPF}_6\text{ (e)}$$

$$\text{TMADH(e). FPF}_6 \underset{k_b'}{\overset{k_b}{\rightleftharpoons}} \text{TMADH. FPF}_6\text{(e)}$$

and ferricenium hexafluorophosphate implies that the rate constants k_a' and k_b' are essentially zero, consistent with an irreversible reaction. The concentration of ferricenium hexafluorophosphate (500 μM; approx. 20 times greater than K_m) used in the kinetic measurements is saturating with respect to enzyme, and therefore, the measured rates of reaction are a direct measure of the slow rate-determining electron transfer rates k_a and k_b from substrate-reduced trimethylamine dehydrogenase to ferricenium hexafluorophosphate (see below for the derivation of the rate equation). In reactions performed with ferricenium hexafluorophosphate concentrations greater than 500 μM, the measured rate constants were found to be similar to those determined at 500 μM ferricenium hexafluorophosphate. The rate constants measured at 500 μM are therefore limiting values. Also, for two-electron-reduced trimethylamine dehydrogenase, following the first fast electron transfer from the reduced flavin to 4Fe-4S center and then to ferricenium hexafluorophosphate the second electron must pass from the flavin to the oxidized 4Fe-4S center before the second transfer to ferricenium hexafluorophosphate. The rate constant for this intramolecular electron transfer from the flavin to the iron–sulfur center at pH 7.0 is >300 s^{-1} (Rohlfs & Hille, 1991) and is much faster than either of the electron transfer rates from the iron–sulfur center to ferricenium hexafluorophosphate (see below). For this reason, this rapid intramolecular electron transfer, which reduces the iron sulfur center with a second electron, is not taken into account in the derived rate equations, as it is much too rapid to affect the kinetic measurements.

For a sequential reaction in which a single electron is passed to ferricenium hexafluorophosphate with rate constants k_a and k_b (Scheme 1), the following rate equations apply:

$$\frac{d[A]}{dt} = -k_a[A] \quad (4)$$

$$\frac{d[B]}{dt} = k_a[A] - k_b[B] \quad (5)$$

where [A] = [TMADH(2e)] and [B] = [TMADH(e)]. Integrating,

$$[A]_t = [A]_o \exp(-k_a t) \quad (6)$$

$$[B]_t = [A]_o[k_a/(k_b - k_a)](e^{-k_a t} - e^{-k_b t}) \quad (7)$$

The rate of production of reduced ferricenium hexafluorophosphate is given by the following relationship:

$$\frac{d[F]}{dt} = k_a[A]_t + k_b[B]_t \quad (8)$$

Substituting,

$$= k_a[A]_o e^{-k_a t} + k_b[A]_o[k_a/(k_b - k_a)](e^{-k_a t} - e^{-k_b t})$$

$$= [A]_o k_a\{[1 + k_b/(k_b - k_a)]e^{-k_a t} - [k_b/(k_b - k_a)]e^{-k_b t}\}$$

Integrating,

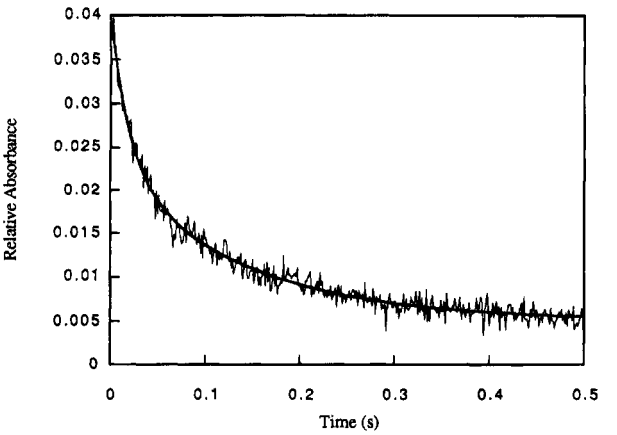

FIGURE 2: Kinetic transient (average of 10 reactions) for the reduction of ferricenium hexafluorophosphate by substrate-reduced trimethylamine dehydrogenase. Absorbance changes were recorded at 347 nm and 20 °C, and reaction components were contained in 20 mM potassium phosphate buffer, pH 7.0. The concentration of substrate-reduced trimethylamine dehydrogenase was 41 μM, and the concentration of ferricenium hexafluorophosphate was 500 μM. The solid line represents the nonlinear least squares fit to the experimental data using eq 9. Amplitude changes are consistent with the expected change in absorbance calculated from the extinction of ferricenium hexafluorophosphate at 347 nm.

$$[F]_t = [A]_o k_a\{-1/k_a[1 + k_b(k_b - k_a)]e^{-k_a t} + [1/(k_b - k_a)]e^{-k_b t}\} + F_o$$

$$[F]_\infty = 2\,[A]_o \rightarrow F_o = 2\,[A]_o$$

The final integrated rate equation is

$$[F]_t = [A]_o\{2 - [(2k_b - k_a)/(k_b - k_a)]e^{-k_a t} + [k_a/(k_b - k_a)]e^{-k_b t}\} \quad (9)$$

Data from the stopped-flow experiments were fitted by nonlinear least squares regression analysis to eq 9, incorporating an offset value to account for a nonzero baseline. A typical reaction progress curve is illustrated in Figure 2. Amplitude changes were, as expected, about 0.04 absorbance unit. Steady-state conditions do not apply for the reaction since no lag phase was observed in the early parts of the progress curve, and our rapid equilibrium assumptions are therefore valid.

At 20 °C, the value of k_a was measured as 49 s^{-1}, which is 7 times greater than the value for k_b measured as 7.3 s^{-1}. The measured values for k_a and k_b are averages of 10 estimations; the standard errors in k_a were less than 7%, and those for k_b were less than 3%. Errors in k_a are somewhat higher than those in k_b because in a double-exponential fit less data is collected in the early part of the progress curve, which is dominated by the k_a term. The observation that k_b is approximately equal to the value of apparent k_{cat} determined under steady-state conditions at the same temperature and pH used for the stopped-flow analyses means that the second electron transfer from the 4Fe-4S center to ferricenium ions may be a candidate for the rate-determining step in overall catalysis. However, it is important to note that the k_{cat} measured is an apparent value and that the true value is likely to be greater than the value presented here. Processes associated with the reductive half-reaction of trimethylamine dehydrogenase may also be rate-limiting

under conditions of excess substrate. These involve the relatively slow binding of a second molecule of trimethylamine to the two-electron-reduced enzyme and the decay of a covalent intermediate which give rise to the $g = 4$ EPR signal (R. J. Rohlfs and R. Hille, manuscript submitted). The slow kinetic phases of the reductive half-reaction are not visible in our experiments since the enzyme is reduced prior to the stopped-flow analyses.

Analysis of Electron Transfer by Temperature Perturbation Studies. The variation with temperature of the rate of electron transfer from the 4Fe-4S center to ferricenium ions was studied by performing stopped-flow reactions at 10, 20, 30, and 40 °C. A relatively large temperature dependence was seen for k_b. The effect of temperature on k_a was less pronounced, and values were found to be in the region of 45−60 s^{-1}. The magnitude of the errors (±7%) for k_a coupled with the observed smaller temperature perturbation effects did not allow rigorous temperature analyses of this rate constant to be undertaken. In contrast, a combination of large temperature-dependent perturbations in the value of k_b and the acquisition of good quality data for k_b allowed the data to be fitted to the classical Marcus equations (eqs 1 and 3). The values of k_b ranged from 5.7 s^{-1} (10 °C) to 19.2 s^{-1} (40 °C). Standard errors were below 3% for averaged sets of data at any one temperature. The fact that different values for k_a and k_b were obtained suggests that the minimal kinetic model (Scheme 1) is too simplistic for describing the electron transfer reactions between the 4Fe-4S center and ferricenium ions. The data, however, are consistent with there being two different electron transfer reactions occurring to two different ferricenium ions bound at different (and perhaps neighboring) sites. This scenario would seem highly plausible, given that the ferricenium ion is not the physiological electron acceptor and consequently lacks a well-defined binding site on the surface of trimethylamine dehydrogenase. Using the measured redox potential for the $4Fe\text{-}4S_{red}/4Fe\text{-}4S_{ox}$ couple of 0.102 V (Barber et al., 1988) and the redox potential for the $ferricenium_{red}/ferricenium_{ox}$ couple of 0.380 V (Lehman et al., 1990), the $\Delta G°$ for the reaction was calculated to be −26.8 kJ/mol. A complication which may arise is the possible temperature dependence of $\Delta G°$ from temperature-dependent conformational changes of trimethylamine dehydrogenase. Acknowledging that there may be temperature dependent fluctuations in $\Delta G°$, given the large value of λ and the nature of the Marcus equations, any change in $\Delta G°$ as a result of temperature perturbation would have to be substantial to compromise our analysis presented here. A nonlinear least squares fit of the data to eq 3 (Figure 3) yielded 13 ± 0.7 Å for the tunneling pathway distance and 183 ± 11 kJ/mol (1.95 eV) for the reorganizational energy. A β value of 1.4 $Å^{-1}$ (Moser et al., 1992) was used in the fit to eq 3. A β value of 0.7 $Å^{-1}$, which is the value that corresponds to a tunneling pathway comprising entirely covalent connectivities (Moser et al., 1992), yielded a tunneling pathway length of 23 ± 0.7 Å. A fit to eq 1 yielded a plot identical to that illustrated in Figure 3 and a value of 0.26 ± 0.15 cm^{-1} for H_{AB}.

Structural Analysis of the Tunneling Pathway. The availability of a high-resolution structure for trimethylamine dehydrogenase (Lim et al., 1986; F. S. Mathews, unpublished work) and a measured value for the electron tunneling pathway distance between the 4Fe-4S center and ferricenium ions have enabled us to identify potential electron tunneling pathways between the redox centers. The shortest distance between the 4Fe-4S center of trimethylamine dehydrogenase and the surface of the protein is 11.6 Å and leads to the hydroxyl of Tyr-442 (Figure 4). This agrees reasonably well with the distance for the electron tunneling pathway (13 ± 0.7 Å; $\beta = 1.4$ $Å^{-1}$) calculated using the kinetic approach described above.

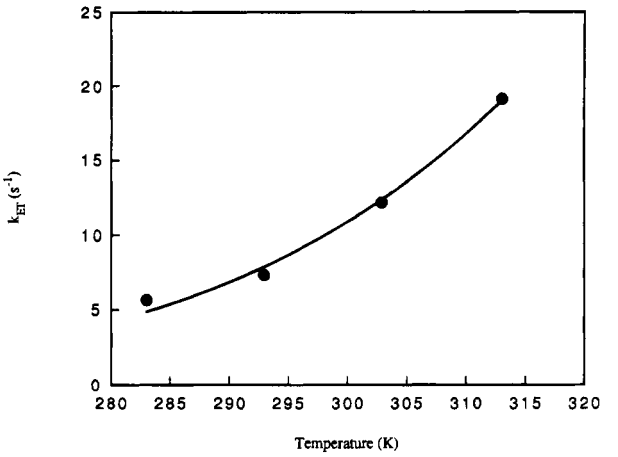

FIGURE 3: Dependence of the second electron transfer rate (k_b) on temperature. Averaged transfer rates and sample size (n) at each temperature are as follows: 10 °C, $k_b = 5.66 \pm 0.14$ ($n = 33$); 20 °C, $k_b = 7.29 \pm 0.23$ ($n = 10$); 30 °C, $k_b = 12.14 \pm 0.15$ ($n = 44$); 40 °C, $k_b = 19.15 \pm 0.6$ ($n = 22$). The solid line represents the fits of the values for k_b to the classical Marcus equations, eqs 1 and 3 (regression coefficient, $R = 0.995$). Fits to the two equations are superimposable.

The pathway distance we have measured from the crystallographic coordinates of trimethylamine dehydrogenase is the shortest distance from the iron−sulfur cluster to the surface of the protein, and it is, therefore, a rather crude structural determination of the tunneling pathway distance. We have made no attempt at this stage to model realistic tunneling routes by maximizing the number of "through-bond" connectivities and minimizing the "through-space" jumps. In reality, tunneling pathways will, to a certain extent, trade less favorable through-space connectivities for longer through-bond connectivities to optimize the value of H_{AB} and the electron transfer rate. The most favored tunneling pathway(s) will probably be slightly longer than the 11.6 Å measured above from the crystallographic coordinates. In our kinetic analyses, by adopting a value for β of 1.4 $Å^{-1}$ (calculated for model protein systems), which is intermediate in value between covalently linked pathways and pathways passing through vacuum, we have attempted to address the heterogeneity found in protein-based electron tunneling pathways by averaging the properties of the bridge material. It might be argued, therefore, that the kinetically determined pathway length of 13 ± 0.7 Å is a more realistic determination of the length of the tunneling pathway which reflects a compromise in optimizing H_{AB} while at the same time minimizing the pathway distance in tunneling from the iron−sulfur cluster to the surface of the protein.

The pathway distance calculated from our kinetic measurements allows us to define an inverted cone whose apex is at the iron ion of the cluster which is closest to the surface of the protein, and whose base forms a small "reactive surface" of about 100 $Å^2$, centered around the side chain of

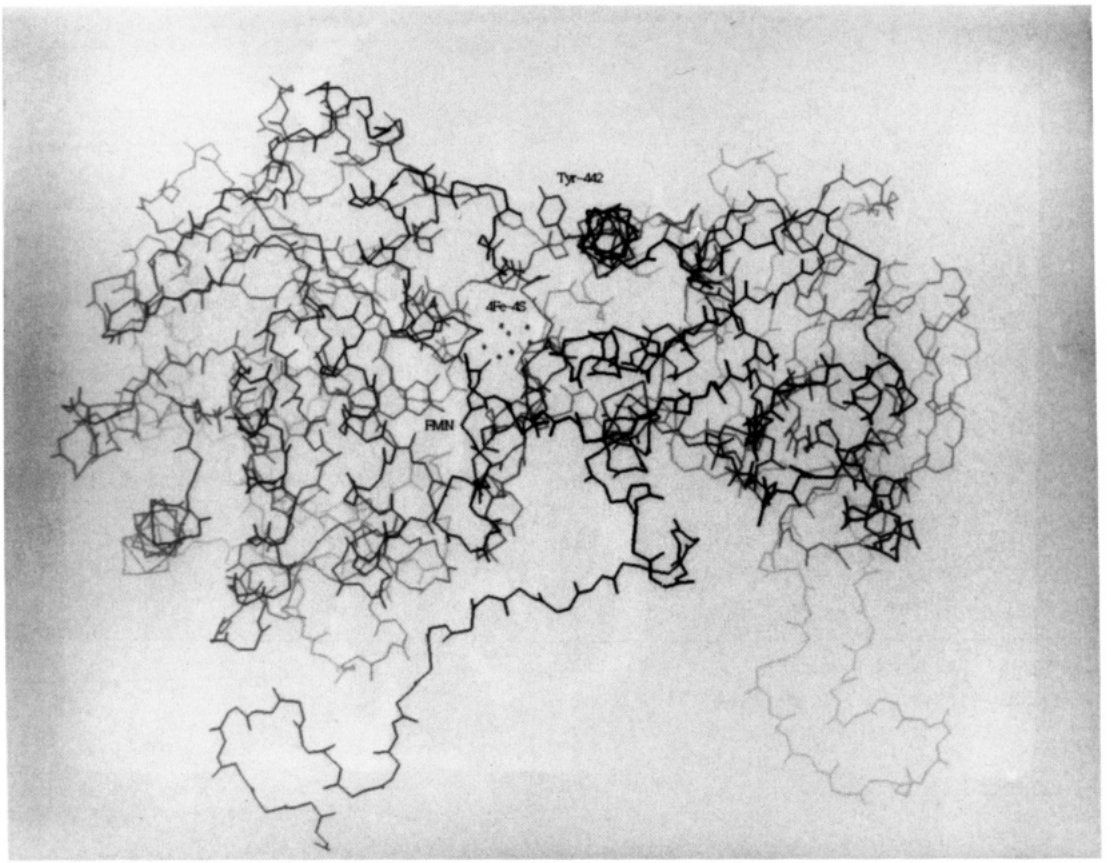

FIGURE 4: Molecular graphics representation of the tunneling pathway from the 4Fe-4S center to the surface of the protein (Tyr-442) in one subunit of trimethylamine dehydrogenase. The FMN and 4Fe-4S center are depicted, and the shortest path distances between the FMN and 4Fe-4S center and also the 4Fe-4S center and the hydroxyl of Tyr-442 are shown. All side chains are omitted with the exception of the side chain for residue Tyr-442. The representation is generated from the refined crystallographic coordinates of trimethylamine dehydrogenase determined at a resolution of 2.4 Å (F. S. Mathews and S. A. White, unpublished work).

Tyr-442. A solvent-accessible surface for the residues in the putative "reactive surface" is displayed in Figure 5. This area was calculated by highlighting all solvent-accessible residues at a distance of 13 Å or less from the iron ion of the cluster whose position is closest to the surface of the protein. Given that electron transfer is not unidirectional and may meander slightly to optimize H_{AB}, one can intuitively see that electron transfer is more likely to occur from the center of the reactive surface rather than the extremities. Naturally, the size of the reactive surface is under the influence of the electronic decay factor β, and therefore, the size of the putative reactive surface may vary depending on the value of β selected. For this reason, the concept of a reactive surface is helpful in visualizing the transfer event but, at this stage and in the absence of further substantiating evidence, we feel unable to place too much prominence on the size and properties of the calculated surface.

Tyrosine 442 within the reactive surface is located at the center of a larger concave region on the surface of the enzyme of approximate dimensions 1200 Å^2 (Figure 4). We speculate that this concave region on the protein surface forms the docking site for the physiological electron acceptor of trimethylamine dehydrogenase which is an FAD-containing electron transfer flavoprotein (ETF). The tunneling pathways used to transfer electrons to ferricenium ions, therefore, may also be exploited in the channeling of electrons to ETF.

DISCUSSION

Previous stopped-flow and freeze−quench kinetic studies of the reaction catalyzed by trimethylamine dehydrogenase have concentrated on the reductive half-reaction and intramolecular electron transfer between the enzyme-bound FMN and the 4Fe-4S center (Steenkamp et al., 1978a,c; Singer et al., 1980; Steenkamp & Beinert, 1982a,b). These studies were conducted under pseudo-first-order conditions, and the reactions were initiated by mixing anaerobic oxidized enzyme with excess trimethylamine. Under these conditions, three kinetic phases were observed: a rapid reduction of the flavin ($\gg k_{cat}$) which is dependent on substrate concentration and two slower kinetic phases ($\sim k_{cat}$) which are independent of substrate concentration. These slower kinetic phases give rise to a $g = 4$ EPR signal and absorbance changes at 365 and 520 nm and are thought to reflect intramolecular electron transfer from flavin to the 4Fe-4S center. For enzyme reduced at the level of two electrons with dithionite, pH jump experiments have demonstrated that intramolecular electron transfer is pH dependent, but more importantly, in the absence of substrate or products, the rate of intramolecular electron transfer is about 100 times greater than k_{cat} (Rohlfs & Hille, 1991). Intramolecular electron transfer is therefore not intrinsically rate-limiting in the absence of substrates or products. Recently, Rohlfs and Hille (1995), using the nonphysiological substrate diethylmethylamine, demonstrated that the breakdown of a covalent substrate−flavin intermediate contributes to the slower kinetic phase of the reductive

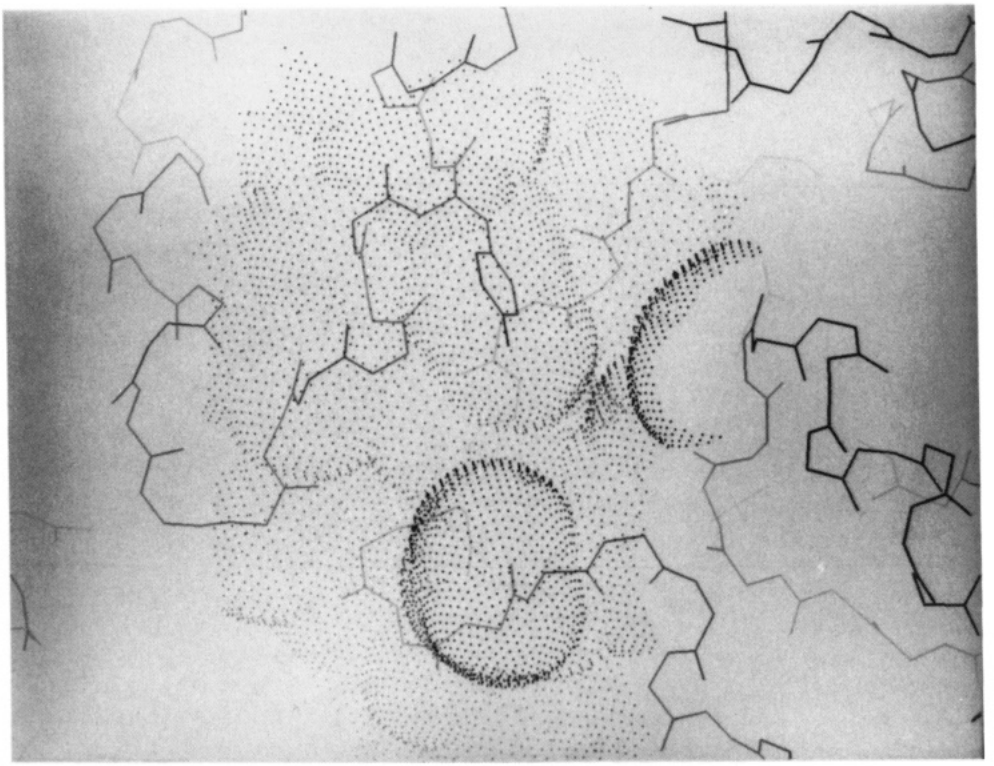

FIGURE 5: The solvent-accessible putative reactive surface surrounding residue Tyr-442 in trimethylamine dehydrogenase. The side chain of tyrosine 442 is shown, and other residues in the reactive surface are depicted as backbone atoms only. Dots correspond to the solvent-accessible surfaces. The solvent-accessible reactive surface was calculated by displaying all solvent accessible areas at a distance of 13 Å or less from the iron ion in the 4Fe-4S cluster which is nearest to the surface of the protein. The kinetically determined tunneling pathway distance (13 Å; $\beta = 1.4$ Å^{-1}) was used to define the solvent-accessible reactive surface.

half-reaction. Since intramolecular electron transfer cannot occur until the covalent intermediate decays, this provides an explanation for the slower rate of intramolecular electron transfer in kinetic experiments utilizing excess substrate compared with those experiments using dithionite-reduced trimethylamine dehydrogenase. They have also demonstrated (under conditions of excess substrate) that the release of product and the binding of a second substrate molecule contribute to the development of the $g = 4$ EPR signal which is reflected in the slower kinetic phase.

The slower kinetic phases associated with the reductive half-reaction do not complicate our experiments on intermolecular electron transfer between the 4Fe-4S center and ferricenium ions. Enzyme is reduced with a stoichiometric amount of trimethylamine prior to the reaction in the stopped-flow apparatus. Consequently, the covalent intermediate formed in the reductive half-reaction has decayed before the transfer reaction is initiated, and the intrinsically fast intramolecular electron transfer between the reduced flavin and the 4Fe-4S center (>300 s^{-1}) is not slowed by the breakdown of the intermediate. Also, by using stoichiometric rather than excess amounts of substrate, the complications arising from the binding of a second molecule of trimethylamine in the active site are negated. The transients observed in the stopped-flow reactions were best fitted to a double-exponential expression consistent with there being two single electron transfers between trimethylamine dehydrogenase and ferricenium ions. The first electron transfer rate is about 7 times faster than the rate of the second electron transfer. The two observed rates may indicate that different electron transfer reactions occur to two ferricenium ions bound at nonequivalent sites.

Values for H_{AB} and λ have been measured for a variety of artificial and physiological long-range electron transfer systems. Several intramolecular electron transfer systems have been studied; a value of 0.7 eV for λ in the bacterial photosynthetic reaction center (Moser et al., 1992) and values in the range 0.8−1.3 eV for λ have been reported for ruthenated proteins (Thieren et al., 1990). More data is gradually becoming available for intermolecular electron transfer between associating proteins. A λ of 0.9 eV has been reported for the cytochrome c−cytochrome b_5 complex (McLendon, 1988; Simmons et al., 1993) and a λ of 1.4 eV has been reported for cytochrome c-cytochrome c peroxidase electron transfer. Harris and Davidson (1993) measured a λ of 1.9 eV for the electron transfer between methanol dehydrogenase and cytochrome c551i. Also, a λ of 2.3 eV has been reported for the reaction between methylamine dehydrogenase and amicyanin (Brooks & Davidson, 1994). These relatively large values for λ were justified by invoking conformational changes after binding or rearrangement of the two proteins to provide the optimal configuration for electron transfer. The large value of λ (1.95 eV) measured in this study for the electron transfer between trimethylamine dehydrogenase and ferricenium ions is comparable to the value of the reorganizational energy measured for inter-protein electron transfer between methanol dehydrogenase and cytochrome c551i, although it seems unlikely that substantial protein rearrangement occurs on binding in the trimethylamine dehydrogenase/ferricenium system. The electron transfer between substrate-reduced trimethylamine dehydrogenase and ferricenium ions is therefore in the low driving force regime ($-\Delta G° \ll \lambda$), and this is manifested in relatively slow electron transfer rates. Our value for H_{AB}

(0.26 cm^{-1}) is within the range of values calculated for other model systems, for example, ruthenated cytochrome *c* molecules (Onuchic et al., 1992).

The tunneling pathway distance (13 ± 0.7 Å) for trimethylamine dehydrogenase predicted from Marcus theory is consistent with the transfer of electrons from the 4Fe-4S center via a "shortest path route" to the surface of the enzyme. In modeling studies, uncertainty exists as to precisely how tunneling pathway distances are measured, particularly in defining the edge of the redox center (Farid et al., 1993). Our "shortest pathway" extends from the phenolic hydroxyl of Tyr-442 located on the surface of the protein to the closest iron ion of the 4Fe-4S center, a distance of 11.6 Å . The structural pathway implies that Tyr-442 plays a role in transferring electrons from trimethylamine dehydrogenase to ferricenium ions, and it is therefore an attractive target for future directed mutagenesis experiments. The residue is located at the center of a large concave region on the surface of trimethylamine dehydrogenase which may form the docking site for the physiological electron acceptor ETF, a postulate which can also be verified by appropriate mutagenesis experiments.

Detailed crystal structures for physiological and soluble electron transfer partners have only been solved for cytochrome *c*—cytochrome *c* peroxidase (Pelletier & Kraut, 1992) and the binary and ternary complexes of methylamine dehydrogenase—amicyanin (Chen et al., 1992) and methylamine dehydrogenase—amicyanin—cytochrome *c*551i (Chen et al., 1994). The structural features which facilitate interprotein electron transfer will only become apparent as more soluble redox complexes are solved. Attempts to crystallize the physiological electron acceptor (ETF) of trimethylamine dehydrogenase and the complex between ETF and the enzyme are in progress. The expectation is that the tunneling pathway used for electron transfer to ferricenium ions is also used for electron transfer to ETF. If so, then the analysis of electron tunneling from the redox centers in wild-type and mutant trimethylamine dehydrogenases to ferricenium ions will be informative and of physiological relevance. Future work will focus on detailed analyses of electron tunneling pathways from the iron—sulfur center to ferricenium ions using algorithms which optimize the tunneling matrix element and predict the most favored routes followed by electrons during the transfer event. Site-directed mutagenesis/kinetic analyses will then be employed to test the predictions generated by the computational methods.

ACKNOWLEDGMENT

We thank Drs A. R. C. Raine and D. S. Bendall for valuable discussion.

REFERENCES

Barber, M. J., Pollock, V., & Spence, J. T. (1988) *Biochem. J. 256*, 657–659.

Barber, M. J., Neame, P. J., Lim, L. W., White, S., & Mathews, F. S. (1991) *J. Biol. Chem. 267*, 6611–6619.

Beratan, D. N., Betts, J. V., & Huddleston, R. K. (1991) *Science 252*, 1285–1288.

Beratan, D. N., Betts, J. N., & Onuchic, J. N. (1992) *J. Phys. Chem. 96*, 2852–2855.

Boyd, G., Mathews, F. S., Packman, L. C., & Scrutton, N. S. (1992) *FEBS Lett. 308*, 271–276.

Brooks, H. B., & Davidson, V. L. (1994) *Biochemistry 33*, 5696–5701.

Chen, L., Durley, R., Poliks, B. J., Hamada, K., Chen, Z., Mathews, F. S., Davidson, V. L., Satow, Y., Huizinga, E., Vellieux, F. M. D., & Hol, W. G. J. (1992) *Biochemistry 31*, 4959–4964.

Chen, L., Durley, R. C. E., Mathews, F. S., & Davidson, V. L. (1994) *Science 264*, 86–90.

Farid, R. S., Moser, C. C., & Dutton, P. L. (1993) *Curr. Opin. Struct. Biol. 3*, 225–233.

Harris, T. K., & Davidson, V. L. (1993) *Biochemistry 32*, 14145–14150.

Hill, C. L., Steenkamp, D. J., Holm, R. H., & Singer, T. P. (1977) *Proc. Natl. Acad. Sci. U.S.A. 74*, 547–551.

Kenney, W. C., McIntire, W., Steenkamp, D. J., & Benisek, W. F. (1978) *FEBS Lett. 85*, 137–139.

Lehman, T. C., Hale, D. E., Bhala, A., & Thorpe, C. (1990) *Anal. Biochem. 186*, 280–284.

Lim, L. W., Shamala, N., Mathews, F. S., Steenkamp, D. J., Hamlin, R., & Xuong, N. (1986) *J. Biol. Chem. 261*, 15140–15146.

Lim, L. W., Mathews, F. S., & Steenkamp, D. J. (1988) *J. Biol. Chem. 263*, 3075–3078.

Marcus, R. A., & Sutin, N. (1985) *Biochim. Biophys. Acta 811*, 265–322.

McLendon, G. (1988) *Acc. Chem. Res. 21*, 160–167.

Moser, C. C., Keske, J. M. Warncke, K., Farid, R. S., & Dutton, P. L. (1992) *Nature 355*, 796–802.

Onuchic, J. N., Beratan, D. N., Winkler, J. R., & Gray, H. B. (1992) *Annu. Rev. Biophys. Biomolec. Struct. 21*, 349–377.

Pelletier, H., & Kraut, J. (1992) *Science 258*, 1748–1755.

Rees, D. C., & Farrelly, D. (1990) in *The Enzymes*, Vol. 19, pp 37–96, Academic Press, Inc., New York.

Rohlfs, R. J., & Hille, R. (1991) *J. Biol. Chem. 266*, 15244–15252.

Rohlfs, R. J., & Hille, R. (1995) *J. Biol. Chem.* (manuscript submitted).

Scrutton, N. S. (1994) *BioEssays 16*, 115–122.

Scrutton, N. S., Packman, L. C., Mathews, F. S., Rohlfs, R. J., & Hille, R. (1994) *J. Biol. Chem.* (in press).

Simmons, J., McLendon, G., & Qiao, T. (1993) *J. Am. Chem. Soc. 115*, 4889–4890.

Singer, T. P., Steenkamp, D. J., Kenney, W. C., & Beinert, H. (1980) in *Flavins and Flavoproteins* (Yagi, K., and Yamano, T., Eds.) pp 277–287, Japan Scientific Societies Press, Tokyo.

Steenkamp, D. J., & Mallinson, J. (1976) *Biochim. Biophys. Acta 429*, 705–719.

Steenkamp, D. J., & Gallup, M. (1978) *J. Biol. Chem. 253*, 4086–4089.

Steenkamp, D. J., & Beinert, H. (1982a) *Biochem. J. 207*, 233–239.

Steenkamp, D. J., & Beinert, H. (1982b) *Biochem. J. 207*, 241–252.

Steenkamp, D. J., Beinert, H., McIntire, W. S., & Singer, T. P. (1978a) in *Mechanisms of Oxidizing Enzymes* (Singer, T. P., & Ondarza, R. N., Eds.) pp 127–141, Elsevier North-Holland Inc., New York.

Steenkamp, D. J., McIntire, W. S., & Kenney, W. C. (1978b) *J. Biol. Chem. 253*, 2818–2828.

Steenkamp, D. J., Singer, T. P., & Beinert, H. (1978c) *Biochem J. 169*, 361–369.

Thieren, M. J., Selman, M. A., Gray, H. B., Chang, I. J., & Winkler, J. R. (1990) *J. Am. Chem. Soc. 112*, 2420–2422.

BI941487P